We are IntechOpen,
the world's leading publisher of Open Access books
Built by scientists, for scientists

4,800
Open access books available

122,000
International authors and editors

135M
Downloads

Our authors are among the

154
Countries delivered to

TOP 1%
most cited scientists

12.2%
Contributors from top 500 universities

CLARIVATE ANALYTICS

BOOK CITATION INDEX

INDEXED

WEB OF SCIENCE™

Selection of our books indexed in the Book Citation Index
in Web of Science™ Core Collection (BKCI)

Interested in publishing with us?
Contact book.department@intechopen.com

Numbers displayed above are based on latest data collected.
For more information visit www.intechopen.com

Applications of Radial Basis Function Schemes to Fractional Partial Differential Equations

Carlos Alberto Torres Martínez and Carlos Fuentes

Additional information is available at the end of the chapter

Abstract

In modeling using diffusion equations, the relationship between fractal geometry and fractional calculus arises by modeling the conditions of the medium as a fractal whose fractional dimension determines the order of this equation. For this reason, it is very useful to have numerical methods that solve them and discretization of the domain is not determinant for the efficiency of the algorithm. In this work, it is proposed to show that meshless methods, in particular methods with radial basis functions (RBF), are an alternative to schemes in differences or structured meshes. We show that we can obtain numerical solutions to some fractional partial differential equations using collocation and RBF, over non equally distributed data.

Keywords: fractional partial differential equations (FPDE), meshless methods, radial basis functions (RBF), Caputo derivative, Riemann-Liouville derivative, Riesz derivative, diffusion-convection

1. Background

1.1. Radial basis function methodology

The Hardy-based radial-based functions (RBF) methodology [1] arises from the need to apply multivariate interpolation to cartography problems, with randomly dispersed data (also known as collocation nodes). Micchelli [2], Powell et al. [3] gave it a great boost by proving non-singularity theorems. Later, Kansa [4, 5] proposed to consider the analytical derivatives of the FBR to develop numerical schemes that deal with partial differential equations (PDE).

Regarding PDE over spaces of dimension greater than one, we generally opt for finite element (FE) type discretizations on meshes, structured or not; also pseudo spectral (PS) methods through base functions such as Fourier or Chebyshev. The high degree of computational

efficiency in the procedure raises the cost in the regularity constraints on the form of the computational domain.

The FE methods involve decomposition of the domain; for example, in two dimensions rectangles are constructed with curvilinear mappings that allow the refinement of the mesh in critical areas. However, this type of implementation is complex and very close nodes are needed, mainly at the domain boundaries, which impairs stability conditions in time.

For this reason, we look for numerical techniques that do not depend to a great extent on data distribution. RBF collocation methods belong to the "meshfree" methods; that is, they only require scattered collocation nodes on the domain and the boundary. They are also an alternative for dealing with problems in larger dimensions and irregular domains. Hence, in recent decades, such methods have attracted the attention of researchers in order to solve partial differential equations. See for example: Chen et al. [6].

This type of technique approximates the solution by means of a linear combination of radial basis functions, which are globally defined and of exponential convergence, but they produce dense and badly conditioned interpolation matrices. On the other hand, some RBFs contain a shape parameter, a number that influences the precision of the numerical results [7, 8].

There are algorithms that also produce better conditioned interpolants, even when the shape parameter tends to zero, with a double precision arithmetic. Some of them are: *Contour-Padé* [9] and *RBF-QR* [10]. Related to the latter is the recent RBF-GA [11].

The RBF-QR method provides a numerically more stable alternative for converting basis that are very similar to each other, or almost linearly dependent on a set of scattered nodes, to a very well conditioned base that generates exactly the same space. This method was originally implemented for nodes on the surface of a sphere in Fornberg and Piret [10]. And recently for an arbitrary set of nodes in one, two, and three dimensions [12, 13].

1.2. Fractional calculus and differential equations: about some applications

The growing interest in fractional calculus has been motivated by applications of fractional equations in different fields of research.

One of the applications considered in this work is that of convection-diffusion equations, which appear not only in many applications of models in Physics and Chemistry [14–17], in problems of flow or heat transfer, but also in other fields such as financial [18, 19]. The solution of a convection-diffusion problem can be interpreted as a probability distribution of one or more underlying stochastic processes [18]. The classical diffusion equation (or heat equation) and its Gaussian solution existed long before Einstein established a connection with random walks.

The anomalous diffusion equations, on the other hand, were originally developed from stochastic walks models [20]. The parameters of these equations are uniquely determined by the fractal dimension of the underlying object [21].

Recent applications of these anomalous diffusion-convection models—those related to oil extraction and hydrological models for aquifers, food production and water distribution in large cities, are quite important [22]. Determining the behavior of the fluid inside the reservoir

and the loss of permeability of the medium assists in the investigation of the mechanisms of oil migration. In this context, the geometric and physical interpretation of fractional derivatives in these differential equations is a "ultra slow" or "ultra fast" diffusion.

The relationship between fractal geometry and fractional calculus is given from the consideration that a particle moves in a porous medium with fractal structure [23]. Thus, when considering the derivative over that variable, a fractional derivative is obtained.

Fuentes et al. [24, 25] proposed a model that represents anomalous diffusion of petroleum (very fast or very slow) in three types of medium with different porosities: fractures, vugs and matrix. This model has a dimensionless form, which is seen as

$$(1 - \omega_f - \omega_v)\frac{\partial^{\alpha_1} p_m}{\partial t^{\alpha_1}} = (1 - \kappa_f - \kappa_v)\frac{1}{r}\frac{\partial}{\partial r}\left(r\frac{\partial^{\beta_1} p_m}{\partial r^{\beta_1}}\right) + \lambda_{mf}(p_f - p_m) + \lambda_{mv}(p_v - p_m), \qquad (1)$$

$$\omega_f \frac{\partial^{\alpha_2} p_f}{\partial t^{\alpha_2}} = \kappa_f \frac{1}{r}\frac{\partial}{\partial r}\left(r\frac{\partial^{\beta_2} p_m}{\partial r^{\beta_2}}\right) - \lambda_{mf}(p_f - p_m) + \lambda_{fv}(p_v - p_f), \qquad (2)$$

$$\omega_v \frac{\partial^{\alpha_3} p_v}{\partial t^{\alpha_3}} = \kappa_v \frac{1}{r}\frac{\partial}{\partial r}\left(r\frac{\partial^{\beta_3} p_m}{\partial r^{\beta_3}}\right) - \lambda_{mv}(p_v - p_m) + \lambda_{fv}(p_v - p_f). \qquad (3)$$

This model must be solved for p's (pressure) at time t in the matrix of the medium p_m, the fractured medium p_f, and the vugular medium p_v.

κ represents each permeability tensor, which is assumed to be constant; r is the dimensionless variable related to the ratios of the wellbore. Values λ are dimensionless values and they are defined in terms of transfer coefficients at each interface, the radius of the wellbore, the dynamic viscosity of the fluid and the permeability tensor.

If time orders α's are less than one we say that the process is **subdiffusive** and if it is greater than one it is called **superdiffusive**. Spatial orders β's result from generalizing the classic Darcy law, which corresponds to $\beta = 1$.

The above equations, like the flow equation that considers the medium as a whole, are modified Bessel's equations.

Different porosities imply different fractal dimensions and therefore, fractional derivatives with different orders.

In Fractional Calculus there is not a single definition of derivative and between these definitions, in general, not equivalent to each other. Definitions such as Riemann-Liouville, Riesz, Caputo, Weyl or Grünwald-Letnikov are the most used to model anomalous diffusion, from a porous medium with fractal dimension.

But, fractional equations present serious numerical and mathematical difficulties in the context of diffusion equations. From the computational point of view, the challenge to overcome is to attenuate the numerical cost of the matrices that result in discretizing the problem. The proposal is to consider radial basis interpolators [26], taking into account that the domain geometry does not determine the efficiency of the algorithm and sounds like an immediate alternative for generalizing larger dimensions.

2. Introduction

The objective in this work is to deal with fractional differential operators, using radial basis functions (RBF) and optimizing discretization processes of such fractional operators, through QR matrix decomposition and to attenuate the bad condition due to the shape parameter. With RBF-QR, a very high precision and convergence are obtained without the need to increase a polynomial term to the interpolator [13]. As the computational cost increases, so does the range of problems to which such a technique can be applied.

3. Radial basis function method for interpolation

Definition 1. *Let s be a positive integer, a function $\varphi : \mathbb{R}^s \to \mathbb{R}$ is called **radial** whenever there is a function in one variable $\phi : [0, \infty) \to \mathbb{R}$ such that*

$$\varphi(\mathbf{x}) = \phi(r), \quad where\, r = \|\mathbf{x}\| \tag{4}$$

*and $\| \cdot \|$ is a norm in $\mathbb{R}^s$ (usually the Euclidean standard norm). **Table (1)** shows some examples, about the more used real functions $\phi(r)$.*

A standard interpolator in terms of radial basis functions, given the data u_k, of some real function u, in the corresponding **collocation nodes $\mathbf{x_k}$, $\mathbf{k} = 1, ..., N$**, has the form [13]

$$s_\varepsilon(\mathbf{x}) = \sum_{k=1}^{N} \lambda_k \phi(\varepsilon \|\mathbf{x} - \mathbf{x_k}\|) \tag{5}$$

where ϕ is one real variable function and the constant value ε is called **shape parameter**.

RBF name	RBF $\phi(r)$
Piecewiese smooth, global	
Polyharmonic spline	r^m, $m = 1, 3, 5,...$
	$r^m \ln(r)$, $m = 2, 4, 6,...$
Compact support ('Wendland')	$(1 - \varepsilon r)_+^m p(\varepsilon r)$, p polynomial.
Smooth, global	
Gaussian (GA)	$e^{-(\varepsilon r)^2}$
Multiquadric (MQ)	$\sqrt{1 + (\varepsilon r)^2}$
Inverse quadric (IQ)	$1/(1 + (\varepsilon r)^2)$
Inverse multiquadric (IMQ)	$1/\sqrt{1 + (\varepsilon r)^2}$
Bessel (BE) ($d = 1, 2,...$)	$J_{d/2-1}(\varepsilon r)/(\varepsilon r)^{d/2-1}$

Table 1. Common elections for $\phi(r)$.

Note 1. *The radial basis function (FBR) we will take for the approach and examples is the* **Gaussian function**:

$$\phi(r) = e^{-r^2} \quad r \geq 0. \tag{6}$$

Because it is globally smooth and for which the RBF method can be applied together with QR matrix decomposition [26].

Notation 1. *Considering one dimensional case, we abbreviate $\phi_k(x) := \phi(\varepsilon||x - x_k||)$. Now the interpolator (5) is written as*

$$s_\varepsilon(x) \equiv \sum_{k=1}^{N} \lambda_k \phi_k(x). \tag{7}$$

The unknown coefficients λ_k can be determined by interpolation conditions

$$s_\varepsilon(x_i) = u_i, \quad i = 1, \ldots, N.$$

producing the linear equations system

$$
\begin{aligned}
\lambda_1 \phi_1(x_1) + \cdots + \lambda_N \phi_N(x_1) &= u_1 \\
\vdots \qquad\qquad \vdots \quad &\ \vdots \\
\lambda_1 \phi_1(x_N) + \cdots + \lambda_N \phi_N(x_N) &= u_N
\end{aligned}
$$

which can be described in matrix form

$$
\underbrace{\begin{bmatrix} \phi_1(x_1) & \cdots & \phi_N(x_1) \\ \vdots & \vdots & \vdots \\ \phi_1(x_N) & \cdots & \phi_N(x_N) \end{bmatrix}}_{A} \underbrace{\begin{bmatrix} \lambda_1 \\ \vdots \\ \lambda_N \end{bmatrix}}_{\lambda} = \underbrace{\begin{bmatrix} u_1 \\ \vdots \\ u_N \end{bmatrix}}_{u_X}.
$$

Thus

$$A\lambda = u_X, \quad \text{where } A = \begin{bmatrix} \Phi(x_1)^T \\ \vdots \\ \Phi(x_N)^T \end{bmatrix} \quad \text{and} \quad \Phi(x) := \begin{bmatrix} \phi_1(x) \\ \vdots \\ \phi_N(x) \end{bmatrix}. \tag{8}$$

A is called **Gram matrix**.

4. RBF methodology for the discretization of differential operators

Suppose we want to apply a differential operator $\mathcal{L}$ to the function $u(x)$ in every **evaluation node** from the set $Z = \{z_1, \ldots, z_{N_e}\}$, given the values of the function at collocation nodes $X = \{x_1, \ldots, x_N\}$

$$\mathcal{L}u_Z \approx Du_X. \tag{9}$$

where $\mathcal{L}u_Z = \begin{bmatrix} \mathcal{L}u(z_1) \\ \vdots \\ \mathcal{L}u(z_{N_e}) \end{bmatrix}$ and $u_X = \begin{bmatrix} u(x_1) \\ \vdots \\ u(x_N) \end{bmatrix}$.

Assuming that $\mathcal{L}$ is linear, we apply it to the RBF interpolator, for each of the evaluation nodes, as an approximation to the values of $\mathcal{L}$ in u:

$$
\begin{aligned}
\mathcal{L}s_\varepsilon(z_i) &= \sum_{k=1}^{N} \lambda_k \mathcal{L}\phi_k(z_i), \quad i = 1, 2, \ldots, N_e; \\
\mathcal{L}(s_\varepsilon(z_1)) &= \lambda_1 \mathcal{L}\phi_1(z_1) + \cdots + \lambda_N \mathcal{L}\phi_N(z_1) \\
\vdots \quad &\quad \vdots \quad\quad\quad\quad\quad \vdots \\
\mathcal{L}(s_\varepsilon(z_{N_e})) &= \lambda_1 \mathcal{L}\phi_1(z_{N_e}) + \cdots + \lambda_N \mathcal{L}\phi_N(z_{N_e})
\end{aligned} \tag{10}
$$

which in the matrix form is

$$\mathcal{L}s_\varepsilon = B\lambda \tag{11}$$

where

$$
\mathcal{L}s_\varepsilon = \begin{bmatrix} \mathcal{L}(s_\varepsilon(z_1)) \\ \vdots \\ \mathcal{L}(s_\varepsilon(z_{N_e})) \end{bmatrix}, B = \begin{bmatrix} \mathcal{L}\phi_1(z_1) & \cdots & \mathcal{L}\phi_N(z_1) \\ \vdots & \vdots & \vdots \\ \mathcal{L}\phi_1(z_{N_e}) & \cdots & \mathcal{L}\phi_N(z_{N_e}) \end{bmatrix}.
$$

The coefficient matrix $\lambda = \begin{bmatrix} \lambda_1 \\ \vdots \\ \lambda_N \end{bmatrix}$ is calculated by solving for λ in Eq. (8). In this way, from Eq. (11) we obtain

$$\mathcal{L}s_\varepsilon = (BA^{-1})u_X. \tag{12}$$

Thus, the matrix BA^{-1} is that matrix D which is mentioned in Eq. (9) and that approximates the values of the differential operator applied to the function.

5. Fractional calculus definitions

The definitions shown in this section are based on the texts of Podlubny [27] and Samko [28].

Generalizing the formula of **Cauchy**, we obtain

$$\mathcal{J}^n\big(f(t)\big) := \int \cdots \int_0^t f(\tau)d\tau = \frac{1}{(n-1)!} \int_0^t (t-\tau)^{n-1} f(\tau)d\tau$$

Definition 2. *The* **left-sided Riemann-Liouville fractional integral** *of order α of function $f(x)$ is defined as*

$$^{RL}_aI^\alpha_xf(x) = \frac{1}{\Gamma(\alpha)}\int_a^x (x-\tau)^{\alpha-1}f(\tau)d\tau, \ x > a. \tag{13}$$

Definition 3. *The* **right-sided Riemann-Liouville fractional integral** *of order α of function $f(x)$ is defined as*

$$^{RL}_xI^\alpha_bf(x) = \frac{1}{\Gamma(\alpha)}\int_x^b (\tau-x)^{\alpha-1}f(\tau)d\tau, \ x < b. \tag{14}$$

Based on the definition of fractional integral, the following fractional derivatives are constructed, which we will use in the numerical examples

Definition 4. *The* **left-sided Riemann-Liouville fractional derivative** *of order α of function $f(x)$ is defined as*

$$^{RL}_aD^\alpha_xf(x) = \frac{1}{\Gamma(m-\alpha)}\frac{d^m}{dx^m}\int_a^x (x-\tau)^{m-\alpha-1}f(\tau)d\tau, \ x > a, \tag{15}$$

where $m = \lceil\alpha\rceil$.

Definition 5. *The* **right-sided Riemann-Liouville fractional derivative** *of order α of function $f(x)$ is defined as*

$$^{RL}_xD^\alpha_bf(x) = \frac{(-1)^m}{\Gamma(m-\alpha)}\frac{d^m}{dx^m}\int_x^b (\tau-x)^{m-\alpha-1}f(\tau)d\tau, \ x < b, \tag{16}$$

where $m = \lceil\alpha\rceil$.

Definition 6. [28–30] *The* **Riesz fractional operator** *for α on a finite interval $0 \leq x \leq L$ is defined as*

$$\frac{\partial^\alpha}{\partial|x|^\alpha}f(x,t) = -c_\alpha\left(^{RL}_aD^\alpha_x + ^{RL}_xD^\alpha_b\right)f(x,t), \tag{17}$$

where

$$c_\alpha = \frac{1}{2\cos\left(\frac{\pi\alpha}{2}\right)}, \ \alpha \neq 1, \tag{18}$$

$$^{RL}_aD^\alpha_xf(x,t) = \frac{1}{\Gamma(m-\alpha)}\frac{d^m}{dx^m}\int_a^x (x-\tau)^{m-\alpha-1}f(\tau,t)d\tau, \tag{19}$$

$$^{RL}_xD^\alpha_bf(x,t) = \frac{(-1)^m}{\Gamma(m-\alpha)}\frac{d^m}{dx^m}\int_x^b (\tau-x)^{m-\alpha-1}f(\tau,t)d\tau, \tag{20}$$

where $m = \lceil\alpha\rceil$.

Definition 7. *The* **left-sided Caputo fractional derivative** *of order α of function $f(x)$ is defined as*

$$^C_a D^\alpha_x f(x) = \frac{1}{\Gamma(m-\alpha)} \int_a^x (x-\tau)^{m-\alpha-1} f^{(m)}(\tau) d\tau, \ x > a, \tag{21}$$

and $m = \lceil \alpha \rceil$.

The fact that the derivative of integer order appears within the integral in Definition 7, makes Caputo derivative the most suitable for dealing with initial conditions of the FPDEs.

Definition 8. *The* **right-sided Caputo fractional derivative** *of order α of function $f(x)$ is defined as*

$$^C_x D^\alpha_b f(x) = \frac{(-1)^m}{\Gamma(m-\alpha)} \int_x^b (\tau-x)^{m-\alpha-1} f^{(m)}(\tau) d\tau, \ x < b, \tag{22}$$

and $m = \lceil \alpha \rceil$.

6. Numerical examples

6.1. Fractional partial differential equation with Riesz space fractional derivatives

The equation that we take in this part is the advection-diffusion equation (see [30, 6]).

$$\frac{\partial u(x,t)}{\partial t} = -K_\alpha \frac{\partial^\alpha u(x,t)}{\partial |x|^\alpha}, \ x \in [0, \pi], \ t \in (0, T],$$
$$u(x,0) = u_0(x), \tag{23}$$
$$u(0,t) = u(\pi, t) = 0,$$

where u can be, for example, the concentration of a dissolute substance, K_α the dispersion coefficient and the fractional derivative of Riesz is given with fractional order $1 < \alpha \leq 2$.

Taking advantage of the fact that for RBFs we can consider non-equispaced collocation nodes, we divide the interval $[0, \pi]$ into N nodes, using Chebyshev distribution (see **Figure 1**):

$$x_i = \frac{\pi}{2} \cos(\theta_i) + \frac{\pi}{2}, \ \theta_i = \pi - i \frac{\pi}{N-1}, \ i = 0, 1, \ldots, N-1.$$

The FPDE is solved by the method of lines based on the spatial trial spaces spanned by the Lagrange basis associated to RBFs. The Lagrange basis $L_1(x), \ldots, L_N(x)$ is generated by radial functions $\phi_j(x) = \phi(|x - x_j|)$, $j = 1, 2, \ldots, N$, taking into account the collocation nodes. This is done by solving the system
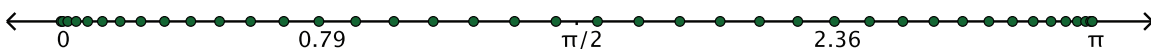
Figure 1. Chebyshev nodes distribution over $[0, \pi]$ interval.

$$L(x)^T = \Phi(x)^T A^{-1} \tag{24}$$

where

$$L(x)^T = [\, L_1(x) \quad \cdots \quad L_N(x) \,], \; \Phi(x)^T = [\, \phi_1(x) \quad \cdots \quad \phi_N(x) \,] \tag{25}$$

and the Gram matrix

$$A = \begin{bmatrix} \phi_1(x_1) & \cdots & \phi_N(x_1) \\ \vdots & \vdots & \vdots \\ \phi_1(x_N) & \cdots & \phi_N(x_N) \end{bmatrix}.$$

If $\mathcal{L}$ is a differential operator and RBF ϕ is sufficiently smooth, then the application of such operator to the Lagrange base is calculated through the relation

$$(\mathcal{L}L)(x) = (\mathcal{L}\phi)A^{-1}.$$

Because of Lagrange's standard conditions, the zero boundary conditions in $x_1 = 0$ and $x_N = \pi$ are de facto fulfilled if we use an approximation generated by the functions $L_2, \ldots, L_{N-1}$. This approximation is then represented as

$$u(x, t) = \sum_{j=2}^{N-1} \beta_j(t) L_j(x),$$

with unknown vector

$$\beta(t) = \begin{bmatrix} \beta_2(t) \\ \vdots \\ \beta_{N-1}(t) \end{bmatrix}.$$

Evaluating the interpolator at the PDE in each node x_i, we obtain

$$\sum_{j=2}^{N-1} \beta_j'(t) L_j(x_i) = -K_\alpha \sum_{j=2}^{N-1} \beta_j(t) \frac{\partial^\alpha}{\partial |x|^\alpha} L_j(x_i)$$

and initial conditions

$$\beta_j(0) = u_0(x_j), \; 2 \leq j \leq N - 1.$$

From the latter two equations we obtain the following system of ordinary differential equations

$$\beta'(t) = -K_\alpha \left(\frac{\partial^\alpha}{\partial |\mathbf{x}|^\alpha} \mathbf{L} \right) \cdot \beta(t), \; \beta(0) = U_0,$$

where

$$\frac{\partial^\alpha}{\partial|\mathbf{x}|^\alpha}\mathbf{L} = \begin{bmatrix} \frac{\partial^\alpha}{\partial|x|^\alpha}L_2(x_2) & \cdots & \frac{\partial^\alpha}{\partial|x|^\alpha}L_{N-1}(x_2) \\ \vdots & \cdots & \vdots \\ \frac{\partial^\alpha}{\partial|x|^\alpha}L_2(x_N) & \cdots & \frac{\partial^\alpha}{\partial|x|^\alpha}L_{N-1}(x_N) \end{bmatrix} \text{ and } U_0 = \begin{bmatrix} u_0(x_2) \\ \vdots \\ u_0(x_{N-1}) \end{bmatrix}. \tag{26}$$

According to the equation data in articles [30, 6], the problem (23) is taken with parameters $\alpha = 1.8$, $K_\alpha = 0.25$ and $u_0(x) = x^2(\pi - x)$. For the numerical solution, Gaussian RBF is used with a shape parameter $\varepsilon = 0.8$, applying the scheme shown in Section 6.1. Graphs are shown in **Figure 2**.
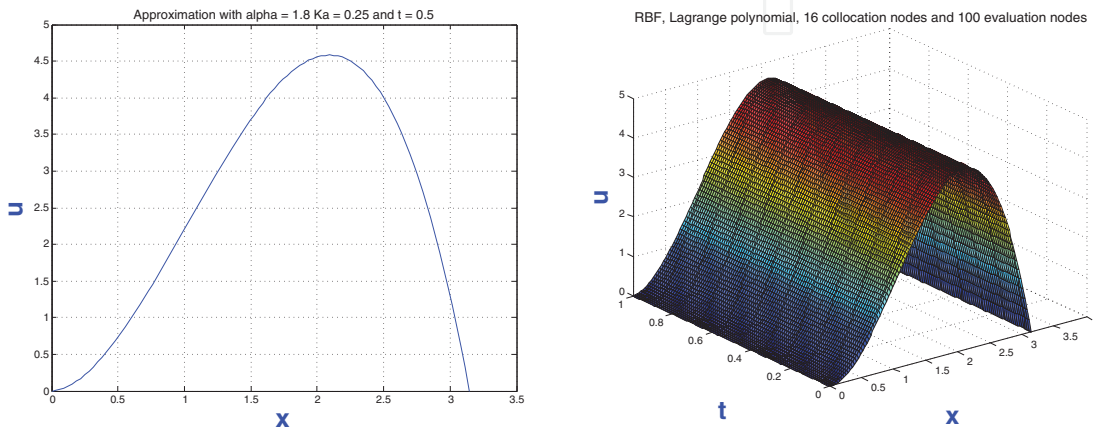
Figure 2. RBF approximation to solution, for Eq. (23), with $\alpha = 1.8$, $\varepsilon = 0.8$ and $K_\alpha = 0.25$.

6.2. Riemann-Liouville space-fractional diffusion equation

In this part we consider the problem introduced by Sousa [31] and taken up in Ref. [26] by Cécile and Hanert, the fractional diffusion equation in one dimension

$$\frac{\partial f(x,t)}{\partial t} = d(x)^{RL}_0 D_x^\alpha f(x,t) + q(x,t), \ x \in [0,1] \text{ and } t > 0 \tag{27}$$

with $^{RL}_0 D_x^\alpha$ Riemannn-Liouville derivative, $1 < \alpha \leq 2$,

$$d(x) = \frac{\Gamma(5-\alpha)}{24}x^\alpha \ y \ q(x,t) = -2e^{-t}x^4.$$

Initial conditions are considered

$$f(x,0) = x^4, \ x \in (a,b) \tag{28}$$

and Dirichlet boundary conditions

$$f(0,t) = 0, \ f(1,t) = e^{-t}. \tag{29}$$

The exact solution to Eq. (27) is

$$f(x, t) = e^{-t}x^4.$$

We apply RBF and the method of lines with Lagrange polynomials, in a similar way as it was applied in Section 6.1. With $N = 21$ Chebyshev collocation nodes and $Ne = 100$ evaluation nodes, various values for the order of the derivative α and for shape parameters.

The results obtained by Sousa [31] were obtained by applying implicit Crank-Nicholson schemes for time. The discretization of the fractional derivative was done using splines, with second-order precision. The results of both Sousa and RBF are shown in **Tables 2** and **3**, taking into account the error

$$||u_{exact} - u_{approximated}||_{\infty} \tag{30}$$

where $|| \cdot ||_{\infty}$ is the ℓ_{∞} norm.

Global ℓ_{∞} error (30) of time converged solution for three mesh resolutions at $t = 1$ for $\alpha = 1.2$, $\alpha = 1.4$ and $\Delta t = \Delta x$.

Δx	$\alpha = 1.2$	Rate	$\alpha = 1.4$	Rate
1/15	0.1275×10^{-2}		0.9070×10^{-3}	
1/20	0.7571×10^{-3}	1.8	0.5327×10^{-3}	1.8
1/25	0.5030×10^{-3}	1.8	0.3486×10^{-3}	1.9
1/30	0.3566×10^{-3}	1.9	0.2461×10^{-3}	1.9

Global ℓ_{∞} error (30) of time converged solution for three mesh resolutions at $t = 1$ for $\alpha = 1.5$, $\alpha = 1.8$ and $\Delta t = \Delta x$.

Δx	$\alpha = 1.5$	Rate	$\alpha = 1.8$	Rate
1/15	0.7660×10^{-3}		0.4380×10^{-3}	
1/20	0.4493×10^{-3}	1.9	0.2540×10^{-3}	1.9
1/25	0.2929×10^{-3}	1.9	0.1649×10^{-3}	1.9
1/30	0.2067×10^{-3}	1.9	0.1150×10^{-3}	2.0

Table 2. Comparison of results for FPDE (27): Sousa results [31].

Global ℓ_{∞} error (30) of time converged solutions at $t = 1$ for $\alpha = 1.2, 1.4, 1.5, 1.8$ and shape parameters $\varepsilon = 0.6, 1.2$.

$\varepsilon = 0.6$		
(r)1-2 Order	**Maximal error**	$\varepsilon = 1.2$
$\alpha = 1.2$	0.35574×10^{-4}	
$\alpha = 1.4$	0.46508×10^{-4}	
$\alpha = 1.5$	0.60498×10^{-4}	
$\alpha = 1.8$	0.16994×10^{-4}	0.18125×10^{-4}

Table 3. Comparison of results for FPDE (27): RBF results.

6.3. Caputo time fractional partial differential equations

In this part we consider examples of fractional partial differential equations (see [32]) of the type

$$\frac{\partial^\alpha u(x, t)}{\partial t^\alpha} + \delta \frac{\partial u(x, t)}{\partial x} + \gamma \frac{\partial^2 u(x, t)}{\partial x^2} = f(x, t), \tag{31}$$

where $t > 0$, $x \in [a, b]$, $0 < \alpha \le 1$, δ and γ are real parameters, bounded initial condition $u(x,0) = u_0(x)$ and Dirichlet boundary conditions $u(a, t) = g_1(t)$ and $u(b, t) = g_2(t)$, $t \ge 0$. Caputo Derivative will be considered and rbf-qr routines from www.it.uu.se/research/scientific_computing/software/rbf_qr

6.3.1. Example 1

Putting $\delta = 1$, $\gamma = -1$ and $f(x, t) = \frac{2t^{2-\alpha}}{\Gamma(3-\alpha)} + 2x - 2$ in Eq. (31), we obtain a non-homogeneous, fractional and linear Burger equation

$$\frac{\partial^\alpha u(x, t)}{\partial t^\alpha} + \frac{\partial u(x, t)}{\partial x} - \frac{\partial^2 u(x, t)}{\partial x^2} = \frac{2t^{2-\alpha}}{\Gamma(3 - \alpha)} + 2x - 2. \tag{32}$$

Using initial condition

$$u(x, 0) = x^2, \tag{33}$$

Dirichlet boundary conditions

$$u(0, t) = t^2, \ u(1, t) = 1 + t^2. \tag{34}$$

The exact solution (see [33]) is

$$u(x, t) = x^2 + t^2, \tag{35}$$

This problem is solved using the method described in section 6.1 along with QR decomposition for spatial part and an implicit scheme for time, on domain $[0, 1]$, fractional derivative of order $\alpha = 0.5$; several shape parameters are considered and the one that gives the best approximation is taken. **Figure 3** shows a 3D image of the solution and maximal error for the solution at time $t = 1$.

In **Figure 4** we compare errors that result when choosing uniform collocation nodes (with a fixed step size) and Chebyshev, on definition interval $[0, 1]$. The election of Chebyshev nodes is due to attenuating instability, which manifests as oscillations in the graph, called the Gibbs phenomenon [34, 35].

[41 uniform collocation nodes and 100 evaluation nodes, maximal error for $t = 0.5$, $\alpha = 0.5$, $\varepsilon = 3.6$ is 0.83595×10^{-4}.] [41 Chebyshev collocation nodes and 100 evaluation nodes, maximal error for $t = 0.5$, $\alpha = 0.5$, $\varepsilon = 3.6$ is 0.14385×10^{-4}.]
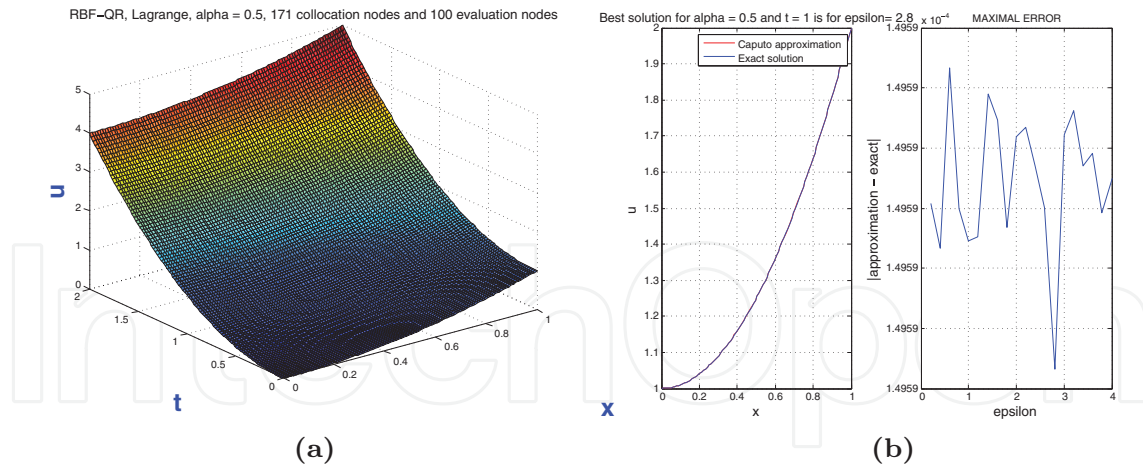
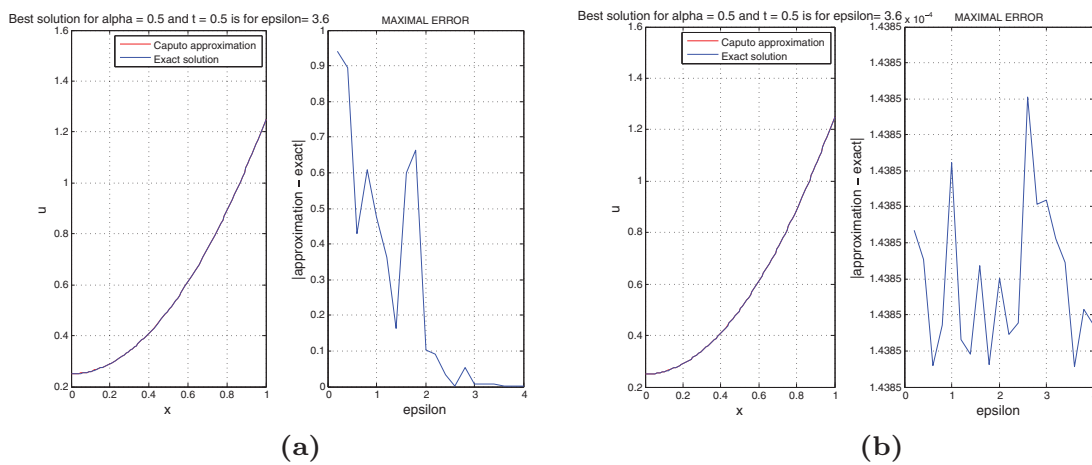**Figure 3.** Numerical solution for Eq. (32) with $\alpha = 0.5$.

Figure 4. Comparison between results for Eq. (32) with $\alpha = 0.5$ and $t = 0.5$, due to election of nodes. (a) 41 uniform collocation nodes and 100 evaluation nodes, maximal error for $t = 0.5$, $\alpha = 0.5$, $\varepsilon = 3.6$ is 0.83595×10^{-4}. (b) 41 Chebyshev collocation nodes and 100 evaluation nodes, maximal error for $t = 0.5$, $\alpha = 0.5$, $\varepsilon = 3.6$ is 0.14385×10^{-4}.

6.3.2. Example 2

Putting $\delta = 1$, $\gamma = 0$ and $f(x, t) = \frac{t^{1-\alpha}}{\Gamma(2-\alpha)} \sin(x) + t \cos(x)$ in Eq. (31), we obtain

$$\frac{\partial^\alpha u(x, t)}{\partial t^\alpha} + \frac{\partial u(x, t)}{\partial x} = \frac{t^{1-\alpha}}{\Gamma(2-\alpha)} \sin(x) + t \cos(x). \tag{36}$$

Initial condition

$$u(x, 0) = 0, \tag{37}$$

Next function is the exact solution (see [33]), which is used to set boundary conditions.

$$u(x, t) = t \sin x. \tag{38}$$

The problem is solved by Lagrange (like Section 6.1) and RBF-QR, for $\alpha = 0.6$, $N = 121$ collocation nodes on interval $[-3, 3]$. In **Figure 5** we notice that when the number of uniform
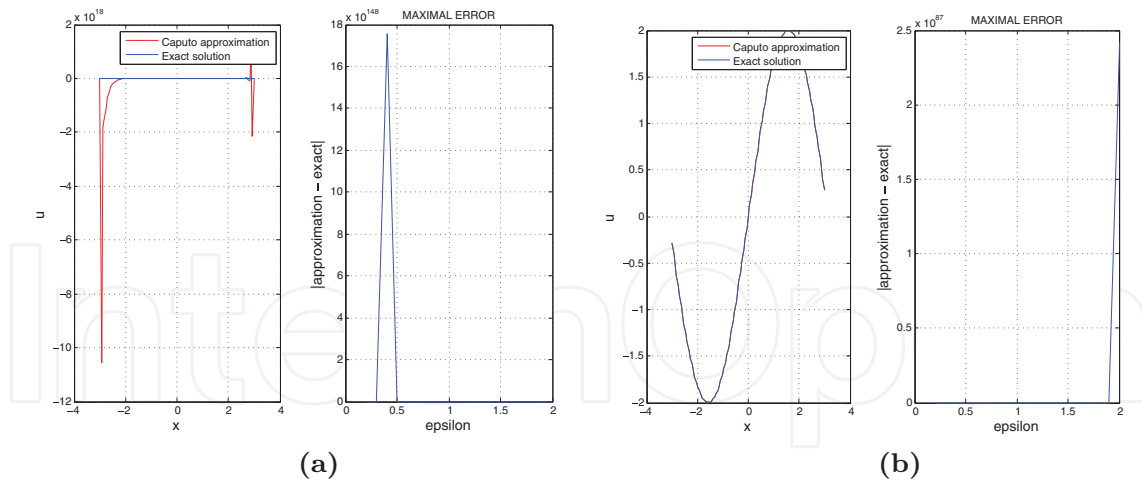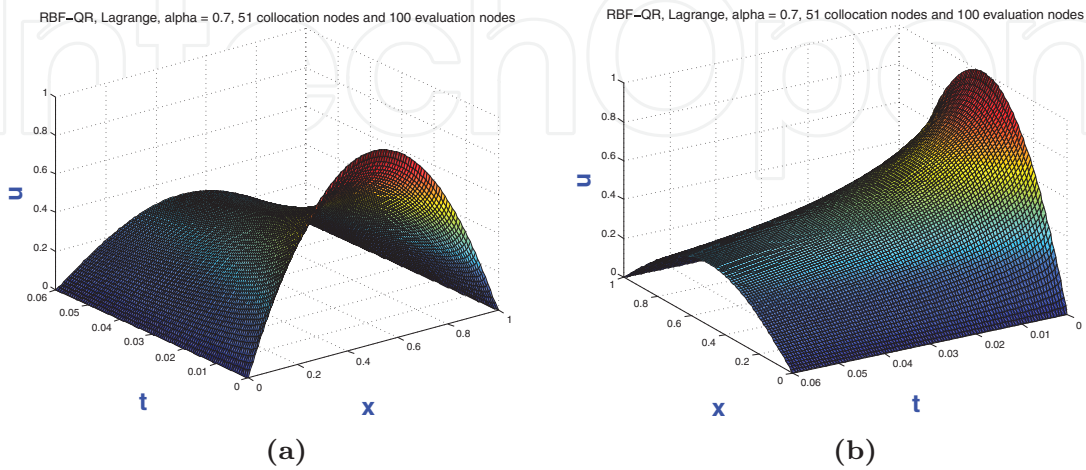
Figure 5. Unstability due to node election, for Eq. (36). (a) 121 uniform collocation nodes and 101 evaluation nodes, maximal error for $t = 2$, $\alpha = 0.6$, $\varepsilon = 1.5$ is 0.10558×10^{19}. (b) 121 Chebyshev collocation nodes and 101 evaluation nodes, maximal error for $t = 2$, $\alpha = 0.6$, $\varepsilon = 0.2$ is 0.71054×10^{-15}.
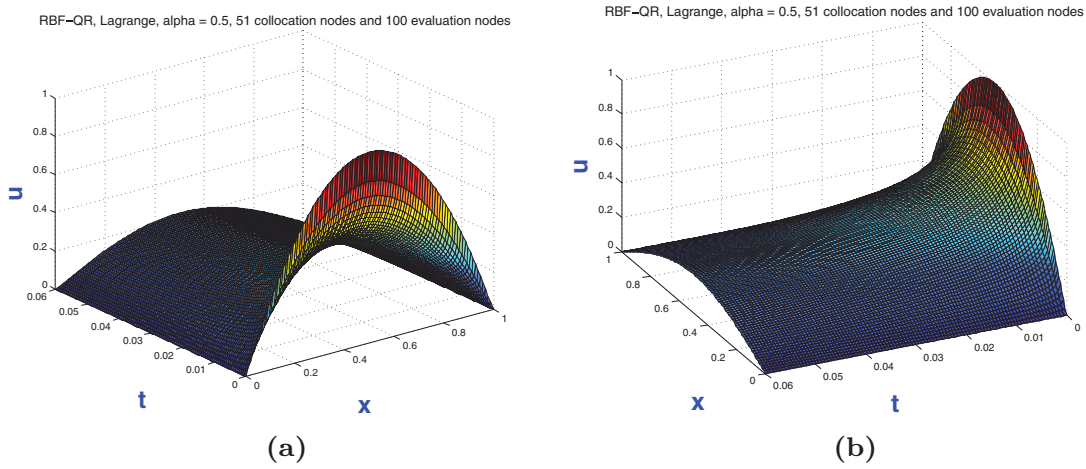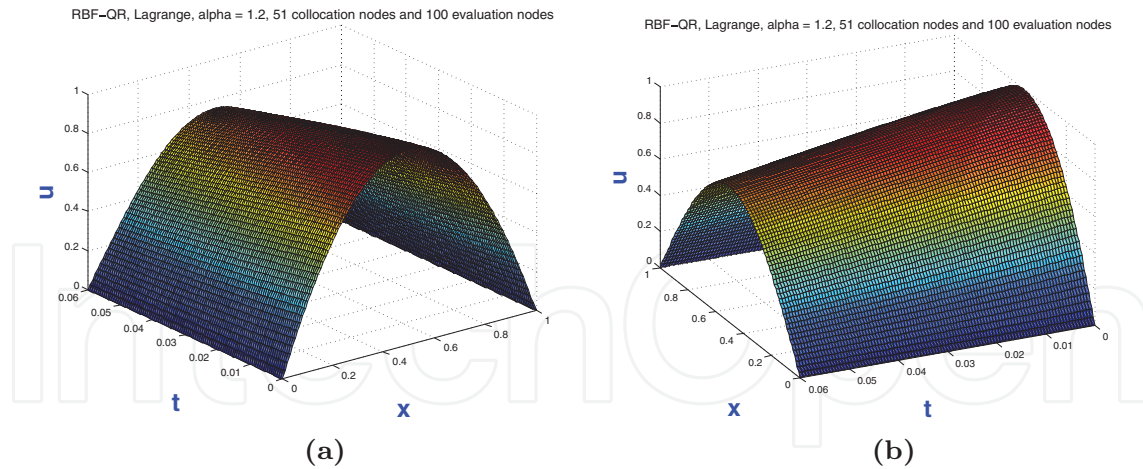

Figure 6. Numerical solution for equation (39), order $\alpha = 0.5$ (superdiffusive phenomenon).

Figure 7. Numerical solution for Eq. (39), order $\alpha = 0.7$ (subdiffusive phenomenon).

Figure 8. Numerical solution for Eq. (39), order $\alpha = 1.2$ (superdiffusive phenomenon).

collocation nodes grows, there are large oscillations which cause unstability. For this reason, Chebyshev nodes are also preferred, as they attenuate this misbehavior.

6.3.3. Example 3

Putting $\delta = 0$, $\gamma = -1$ and $f(x, t) = 0$ in Eq. (31), we obtain

$$\frac{\partial^\alpha u(x, t)}{\partial t^\alpha} = \frac{\partial^2 u(x, t)}{\partial x^2}. \tag{39}$$

using initial condition

$$u(x, 0) = 4x(1 - x), \tag{40}$$

boundary conditions

$$u(0, t) = u(1, t) = 0. \tag{41}$$

The exact solution of this problem is not known, but is shown as an example of subdiffusive phenomenon which was discussed in the introduction. The problem is solved using the method described in section 6.1 along with QR decomposition for spatial part and an implicit scheme for time, on domain $[0, 1]$, fractional derivative of order $\alpha = 0.5$ and $\alpha = 0.7$, according to the results shown in Refs. [36, 32]. **Figures 6** and **7** show these results. **Figure 8** shows a what if situation when $\alpha = 1.2$ (superdiffusive phenomenon), mentioned in Section 1.2.

7. Discussion

The idea was to show that radial basis schemes are efficient and are on par with schemes like Finite Differences. They are an option to deal with multidimensional and irregular domain problems. The challenge is to adapt them to deal with diffusive problems, particularly with

multidimensional systems of equations that consider that the medium does not have a single characteristic.

Fuentes et al. show in the work "The fractal models of saturated and unsaturated flows (capillary, diffusion and matrix) at micro, macro and mega scales", for the PEMEX oil company, how to model the pressure which the oil must leave in a wellbore, from a system of triple porosity and permeability of the fractured medium.

By converting the model into a dimensionless system, in terms of radial distances, non-mesh schemes such as RBFs sound like a viable option and it is a work that is still being addressed.

Author details

Carlos Alberto Torres Martínez[1]* and Carlos Fuentes[2]

*Address all correspondence to: inocencio3@gmail.com

1 Universidad Nacional Autónoma de México, Universidad Autónoma de la Ciudad de México (UACM), Mexico

2 Instituto Mexicano de Tecnología del Agua, Coordinación de Tecnología de Riego y Drenaje, Cuernavaca, Mexico

References

[1] Rolland L Hardy. Multiquadric equations of topography and other irregular surfaces. Journal of geophysical research, 76(8):1905–1915, 1971.

[2] Charles A Micchelli. Interpolation of scattered data: distance matrices and conditionally positive definite functions. In Approximation theory and spline functions pp. 143–145. Springer Netherlands. 1984.

[3] Michael JD Powell. The theory of radial basis function approximation in 1990. Department of Applied Mathematics and Theoretical Physics, University of Cambridge. pp. 105–209. 1990.

[4] Edward J Kansa. Multiquadrics—a scattered data approximation scheme with applications to computational fluid-dynamics—i surface approximations and partial derivative estimates. Computers & Mathematics with applications, 19(8):127–145, 1990.

[5] Edward J Kansa. Multiquadrics—a scattered data approximation scheme with applications to computational fluid-dynamics—ii solutions to parabolic, hyperbolic and elliptic partial differential equations. Computers & mathematics with applications, 19(8):147–161, 1990.

[6] Wen Chen, Zhuo-Jia Fu, and Ching-Shyang Chen. Recent advances in radial basis function collocation methods. Heidelberg: Springer, 2014.

[7]   Marjan Uddin. On the selection of a good value of shape parameter in solving time-dependent partial differential equations using rbf approximation method. Applied Mathematical Modelling, 38(1):135–144, 2014.

[8]   Shmuel Rippa. An algorithm for selecting a good value for the parameter c in radial basis function interpolation. Advances in Computational Mathematics, 11(2-3):193–210, 1999.

[9]   Bengt Fornberg and Grady Wright. Stable computation of multiquadric interpolants for all values of the shape parameter. Computers & Mathematics with Applications, 48(5): 853–867, 2004.

[10] Bengt Fornberg and Cécile Piret. A stable algorithm for flat radial basis functions on a sphere. SIAM Journal on Scientific Computing, 30(1):60–80, 2007.

[11] Bengt Fornberg, Erik Lehto, and Collin Powell. Stable calculation of gaussian-based rbf-fd stencils. Computers & Mathematics with Applications, 65(4):627–637, 2013.

[12] Bengt Fornberg, Elisabeth Larsson, and Natasha Flyer. Stable computations with gaussian radial basis functions. SIAM Journal on Scientific Computing, 33(2):869–892, 2011.

[13] Elisabeth Larsson, Erik Lehto, Alfa Heryudono, and Bengt Fornberg. Stable computation of differentiation matrices and scattered node stencils based on gaussian radial basis functions. SIAM Journal on Scientific Computing, 35(4):A2096–A2119, 2013.

[14] Eli Barkai, Ralf Metzler, and Joseph Klafter. From continuous time random walks to the fractional Fokker-Planck equation. Physical Review E, 61(1):132, 2000.

[15] A Blumen, G Zumofen, and J Klafter. Transport aspects in anomalous diffusion: Lévy walks. Physical Review A, 40(7):3964, 1989.

[16] A Piryatinska, AI Saichev, and WA Woyczynski. Models of anomalous diffusion: the subdiffusive case. Physica A: Statistical Mechanics and its Applications, 349(3):375–420, 2005.

[17] AS Chaves. A fractional diffusion equation to describe lévy flights. Physics Letters A, 239 (1):13–16, 1998.

[18] Ali Safdari-Vaighani, Alfa Heryudono, and Elisabeth Larsson. A radial basis function partition of unity collocation method for convection–diffusion equations arising in financial applications. Journal of Scientific Computing, 64(2):341–367, 2015.

[19] L Sabatelli, S Keating, J Dudley, and P Richmond. Waiting time distributions in financial markets. The European Physical Journal B-Condensed Matter and Complex Systems, 27 (2):273–275, 2002.

[20] Mark M Meerschaert, Jeff Mortensen, and Stephen W Wheatcraft. Fractional vector calculus for fractional advection–dispersion. Physica A: Statistical Mechanics and its Applications, 367:181–190, 2006.

[21] Ralf Metzler, Walter G Glöckle, and Theo F Nonnenmacher. Fractional model equation for anomalous diffusion. Physica A: Statistical Mechanics and its Applications, 211(1):13–24, 1994.

[22] Erika Di Giuseppe, Monica Moroni, and Michele Caputo. Flux in porous media with memory: models and experiments. Transport in Porous Media, 83(3):479–500, 2010.

[23] K Oleschko, G Korvin, AS Balankin, RV Khachaturov, L Flores, B Figueroa, J Urrutia, and F Brambila. Fractal scattering of microwaves from soils. Physical Review Letters, 89 (18):188501, 2002.

[24] C Fuentes, F Brambila, M Vauclin, J-Y Parlange, and R Haverkamp. Fractal modeling of hydraulic conductivity in non-saturated soils. Hydraul. Eng. Mexico, 16 (2):119–137 (in spanish) 2001.

[25] C Fuentes. Approche fractale des transferts hydriques dans les sols non-saturés. These de doctorat de l'Université Joseph Fourier Grenoble I, Grenoble, France, 1992.

[26] Cécile Piret and Emmanuel Hanert. A radial basis functions method for fractional diffusion equations. Journal of Computational Physics, 238:71–81, 2013.

[27] Igor Podlubny. Fractional differential equations: an introduction to fractional derivatives, fractional differential equations, to methods of their solution and some of their applications, volume 198. Academic Press, USA. 1998.

[28] Stefan G Samko, Anatoly A Kilbas, and Oleg I Marichev. Fractional integrals and derivatives. Theory and Applications, Gordon and Breach, Yverdon, 1993, 1993.

[29] Rudolf Gorenflo and Francesco Mainardi. Random walk models for space-fractional diffusion processes. Fractional Calculus and Applied Analysis, 1(2):167–191, 1998.

[30] Qianqian Yang, Fawang Liu, and I Turner. Numerical methods for fractional partial differential equations with riesz space fractional derivatives. Applied Mathematical Modelling, 34(1):200–218, 2010.

[31] Erclia Sousa. Numerical approximations for fractional diffusion equations via splines. Computers & Mathematics with Applications, 62(3):938–944, 2011.

[32] Marjan Uddin and Sirajul Haq. Rbfs approximation method for time fractional partial differential equations. Communications in Nonlinear Science and Numerical Simulation, 16(11):4208–4214, 2011.

[33] Zaid Odibat and Shaher Momani. The variational iteration method: an efficient scheme for handling fractional partial differential equations in fluid mechanics. Computers & Mathematics with Applications, 58(11):2199–2208, 2009.

[34] David Gottlieb and Chi-Wang Shu. On the Gibbs phenomenon and its resolution. SIAM Review, 39(4):644–668, 1997.

[35] Tobin A Driscoll and Bengt Fornberg. A padé-based algorithm for overcoming the Gibbs phenomenon. Numerical Algorithms, 26(1):77–92, 2001.

[36] Igor Podlubny, Aleksei Chechkin, Tomas Skovranek, YangQuan Chen, and Blas M Vinagre Jara. Matrix approach to discrete fractional calculus ii: Partial fractional differential equations. Journal of Computational Physics, 228(8):3137–3153, 2009.